

This is a repository copy of *A high-resolution spatial model to predict exposure to pharmaceuticals in European surface waters – ePiE*.

White Rose Research Online URL for this paper:

<https://eprints.whiterose.ac.uk/136982/>

Version: Accepted Version

Article:

Oldenkamp, Rik, Hoeks, Selwyn, Cenzic, Merza et al. (4 more authors) (2018) A high-resolution spatial model to predict exposure to pharmaceuticals in European surface waters – ePiE. *Environmental science & technology*. pp. 12494-12503. ISSN 1520-5851

<https://doi.org/10.1021/acs.est.8b03862>

Reuse

Items deposited in White Rose Research Online are protected by copyright, with all rights reserved unless indicated otherwise. They may be downloaded and/or printed for private study, or other acts as permitted by national copyright laws. The publisher or other rights holders may allow further reproduction and re-use of the full text version. This is indicated by the licence information on the White Rose Research Online record for the item.

Takedown

If you consider content in White Rose Research Online to be in breach of UK law, please notify us by emailing eprints@whiterose.ac.uk including the URL of the record and the reason for the withdrawal request.

1 Title

2 A high-resolution spatial model to predict exposure to pharmaceuticals in European surface
3 waters – ePiE

4 Authors

5 Rik Oldenkamp^{*1,2}, Selwyn Hoeks¹, Mirza Čengić¹, Valerio Barbarossa¹, Emily E. Burns²,

6 Alistair B.A. Boxall², Ad M.J. Ragas^{1,3}

7 ¹Department of Environmental Science, Radboud University Nijmegen, 6500GL, Nijmegen, The Netherlands

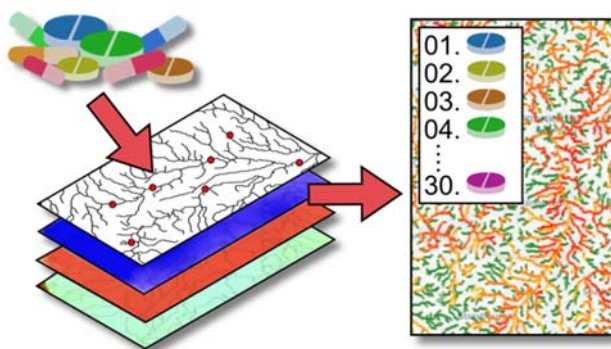
8 ²Environment Department, University of York, Heslington, York YO10 5DD, United Kingdom

9 ³Faculty of Management, Science & Technology, Open Universiteit, Valkenburgerweg 177, 6419 AT Heerlen, The

10 Netherlands

11 * Corresponding author, at r.oldenkamp@science.ru.nl

12 Graphical abstract



13

Abstract

Environmental risk assessment of pharmaceuticals requires the determination of their environmental exposure concentrations. Existing exposure modelling approaches are often computationally demanding, require extensive data collection and processing efforts, have a limited spatial resolution, and have undergone limited evaluation against monitoring data. Here, we present ePiE (exposure to Pharmaceuticals in the Environment), a spatially explicit model calculating concentrations of active pharmaceutical ingredients (APIs) in surface waters across Europe at ~1 km resolution. ePiE strikes a balance between generating data on exposure at high spatial resolution while having limited computational and data requirements. Comparison of model predictions with measured concentrations of a diverse set of 35 APIs in the river Ouse (UK) and Rhine basins (North West Europe), showed around 95% were within an order of magnitude. Improved predictions were obtained for the river Ouse basin (95% within a factor of 6; 55% within a factor of 2), where reliable consumption data were available and the monitoring study design was coherent with the model outputs. Application of ePiE in a prioritisation exercise for the Ouse basin identified metformin, gabapentin, and acetaminophen as priority when based on predicted exposure concentrations. After incorporation of toxic potency, this changed to desvenlafaxine, loratadine and hydrocodone.

Introduction

Over the past decades, human consumption of pharmaceuticals has steadily increased.^{1, 2} In combination with continuing improvements in our analytical capabilities,^{3, 4} this has led to the detection of many active pharmaceutical ingredients (APIs) in surface waters worldwide.^{5, 6} The environmental presence of 631 different pharmaceuticals has been reported in 71 countries covering all continents,⁵ but the actual number of APIs present in surface waters is likely higher due to the self-fulfilling selection bias of many monitoring campaigns.⁷

A crucial step in the environmental risk assessment of chemicals is the determination of their environmental exposure potential. Since there are currently at least 1500 distinct APIs in use,^{8, 9} monitoring all of them everywhere and continuously is practically impossible. Moreover, APIs under development will not be present in the environment so monitoring will provide no information on exposure of these molecules. There is therefore a need for exposure modelling approaches that can help us prioritize our monitoring efforts, support more robust environmental risk assessment of new APIs, and that can be used to take targeted measures.¹⁰ These should preferably be spatially explicit, acknowledging that geographical variability can lead to substantial differences in the concentrations of APIs across and within regions.^{11, 12} For example, rankings of APIs established at the continental European level may lead to misguided allocation of resources when adopted at a regional level.¹² Such mismatches between EU-level and regional level prioritization of APIs might, for example, be the result of geographical variation in API consumption, a heterogeneous distribution of emission sources, or spatially varying environmental conditions driving the fate of APIs after emission.

The environmental exposure potential of chemicals is reflected by the measured (MEC) or predicted (PEC) environmental concentrations at which they occur in the environmental compartment of interest. PECs can be derived using multimedia fate models, such as the EUSES model¹³ and our previously developed prioritization tool for APIs.¹¹ These are based on mass-balance equations for interconnected compartments that represent the relevant environmental media (e.g., fresh and salt waters, air, urban and agricultural soils, et cetera), and are therefore especially useful for larger scale (regional, continental) assessments where multiple media might be relevant. However, they are less suitable for answering locally specific questions (e.g., hotspot identification, scenario analyses for optimal mitigation measures), because they assume a homogenous distribution of chemicals within their compartments and do not account for any spatial variation at that scale.^{14, 15} This also inherently limits the options for model corroboration with local measurement data.

APIs tend to largely remain in the compartment where they are emitted,¹⁶ implying that the use of single-media models is also an option. Examples of geographically-based single-media models for down-the-drain chemicals are GREAT-ER,¹⁷ PhATE,¹⁸ GWAVA,¹⁹ LF2000-WQX,²⁰ iSTREEM,²¹ and the recent unnamed model by Grill et al.¹⁵ Combined, these models have been applied to assess the distribution of APIs in many river basins worldwide. Invariably, they integrate information on API consumption, human metabolism, removal in wastewater treatment plants (WWTPs), and dilution and dissipation in receiving surface waters, to estimate PECs throughout river basins. The characterization of hydrology is broadly done in one of two ways: via gridded approaches incorporating extensive process-based hydrological models,^{15, 19} or via segmentation of the river network into discrete river segments with calibration against measured hydrology and extrapolation to ungauged sites.^{17, 18, 20, 21} Both

approaches have their own drawbacks, related to the computational demands of large scale hydrological models, the extensive data collection and processing efforts required for the parameterization of river basins, and the limited spatial resolution determined by the grid-cell size or the length of individual river segments.

Here, we present ePiE (exposure to Pharmaceuticals in the Environment), a new spatially explicit model, developed in the frame of the Innovative Medicines Initiative iPiE project, that can calculate concentrations of APIs in surface waters throughout river basins in Europe. It is designed to strike a balance between generating data on exposure at high spatial resolution while having limited computational and data requirements. It does so by employing FLO1K for the underlying hydrology, a global geographic dataset with annual predictions of streamflow metrics (annual mean flow, highest and lowest monthly mean flow) spatially distributed at 30 arc seconds (~1 km).²² This is a resolution ten times higher than the most detailed global hydrological models or land surface models currently available.^{23, 24} In ePiE, river networks are represented as collections of interconnected nodes describing emission points, river junctions, river mouths and inlets and outlets of lakes and reservoirs. It thus provides a modelling architecture supporting linkage and integration of geographic information in vector format, i.e., the nodes of the river networks, and rasterized information on climatic, hydrological, and geochemical conditions.²⁵ We developed a custom routing scheme to follow APIs through the river network, along the way accounting for dissipation from the water via the processes of biodegradation, photolysis, hydrolysis, volatilization and sedimentation.

In this article, we present the structure of ePiE and evaluate its performance against measured concentration data from the open literature for a combined total of 35 APIs in two

European river basins. Finally, to illustrate the utility of the model, we apply ePiE to rank APIs in the river Ouse basin (UK), based on predicted concentrations in surface waters and predicted risks to fish.

Methods

Model structure

Central to ePiE are a set of network nodes derived from the global databases HydroSHEDS²⁶ and HydroLAKES,²⁷ and agglomerations and WWTPs from the UWWTD-Waterbase.²⁸ This latter database contains information on the location and characteristics (i.e., generated load, design capacity and level of treatment) of 30,043 European urban WWTPs and 27,695 agglomerations with generated wastewater loads above 2,000 population equivalents (p.e.). After curation of the UWWTD-Waterbase (see Supporting Information S1), agglomerations and WWTPs were incorporated into the river network based on their proximity to the nearest water body. Direct emissions into the sea were excluded from the model. Finally, gridded information on air temperature, wind speed, slope, and streamflow was extracted to all nodes in the network. To optimize its flexibility and accessibility, ePiE is entirely constructed in the open-source software environment R,²⁹ and a description of the model construction can be found in Supporting Information S2.

The ePiE model has a modular structure based on the georeferenced river basins provided by the global HydroBASINS database²⁵ which includes basins below of 60 °N. Depending on the river basin of interest, a subset of the total network of nodes is geographically selected. As a starting point, ePiE then requires yearly consumption data for the API of interest (kg/year) for all countries the river basin covers. When the API of interest is formed as a metabolite from another API, i.e. its prodrug, consumption data for that prodrug are also needed. Yearly

emissions into the river network from WWTPs ($E_{w,wwtp}$; kg/year) and from agglomerations with incomplete WWTP connectivity ($E_{w,agg}$; kg/year) are calculated via Equation 1 and Equation 2, respectively. The country-specific yearly consumption data (M) include the prescription of pharmaceuticals in hospitals. This means that hospital emissions are not included as location-specific point sources, but spatially distributed according to the wastewater loads per agglomeration (i.e., a proxy for population density).

$$E_{w,wwtp} = (M \cdot f_{pc} + M_{pd} \cdot f_{met}) \cdot \frac{\sum_{j=1}^n (V_{ww,agg,j} \cdot f_{conn,agg,j} \cdot f_{wwtp,agg,j})}{V_{ww,cnt}} \cdot (1 - f_{rem}) \quad \text{Equation 1}$$

Where M and M_{pd} are the yearly consumption of the API of interest and its prodrug in the relevant country (kg/year); f_{pc} is the fraction of the administered parent compound excreted/egested unchanged or as reversible conjugates via urine and faeces (-); f_{met} is the fraction of prodrug metabolized to the API of interest, and subsequently excreted/egested via urine and faeces (-); n is the number of agglomerations j connected to the WWTP (-); $f_{conn,agg,j}$ is the level of WWTP connectivity per agglomeration j ; $f_{wwtp,agg,j}$ is the fraction of agglomeration j connected to the WWTP; f_{rem} is the API-specific removal efficiency per WWTP (-); and $V_{ww,agg,j}$ and $V_{ww,cnt}$ are the wastewater loads generated per agglomeration j and the total in the relevant country, respectively (p.e.).

$$E_{w,agg} = (M \cdot f_{pc} + M_{pd} \cdot f_{met}) \cdot \frac{V_{ww,agg} \cdot (1 - f_{conn,agg})}{V_{ww,cnt}} \quad \text{Equation 2}$$

The SimpleTreat 4.0 model³⁰ was incorporated into ePiE to estimate the removal efficiency during wastewater treatment (f_{rem}). It requires basic physicochemical properties as input, as well as solids-water partitioning coefficients for primary sewage (Kp_{ps} ; L/kg) and activated sludge (Kp_{as} ; L/kg), and (pseudo-)first order biodegradation rate constants ($k_{bio,wwtp}$; s⁻¹). Removal efficiencies were assigned to individual WWTPs depending on their associated level of treatment, using either the full SimpleTreat 4.0 model for those employing consecutive primary and secondary treatment, or the module for primary treatment only.

After their emission, API residues are followed through the river network using a routing procedure ordered from the most upstream to the most downstream nodes. As such, the contribution of all upstream emissions to local concentrations is considered. Along the way, ePiE accounts for dilution in the water column and five (pseudo-)first order loss processes, three being degradation processes, i.e. biodegradation, photolysis and hydrolysis, and two being intermedia transport processes, i.e. sedimentation and volatilization. Equation 3 calculates concentration C_i ($\mu\text{g/L}$) at any node i in the river network; Equation 4 calculates concentrations in lakes and reservoirs, following an approach similar to Grill et al.¹⁵ in which they are modelled as single completely stirred tank reactors.

$$C_i = \frac{E_{w,i} + \sum_{j=1}^n \left(E_{w,j} \cdot e^{-\left[\sum_{m=1}^5 k_{m,d_{j-i}} \right] \frac{d_{j-i}}{v_{d_{j-i}}}} \right)}{Q_i} \quad \text{Equation 3}$$

Where $E_{w,i}$ and $E_{w,j}$ are the emissions into the river network at node i and at node j upstream from node i , respectively (mg/s); n is the total number of nodes upstream from node i (-); d_{j-i} is the distance over the river network between node j and node i (m); $k_{m,d_{j-i}}$ is the average (pseudo-) first order rate constant for loss process m over d_{j-i} (s^{-1}); $v_{d_{j-i}}$ is the average river flow velocity over d_{j-i} (m/s); and Q_i is the total river flow at node i (m^3/s), including any discharges.

$$C_i = \frac{\sum_{p=1}^n (E_{w,p})}{(V_i/HRT_i) + \sum_{m=1}^5 (k_{m,i}) \cdot V_i} \quad \text{Equation 4}$$

Where $E_{w,p}$ is the emission into lake or reservoir i coming from node p (mg/s), which can either be a direct emission source (i.e., a WWTP or an agglomeration), or an inlet point carrying API residues from upstream the river network; n is the total number of nodes emitting into lake or reservoir i (-); HRT_i is the hydraulic retention time of lake or reservoir i (s); V_i is the volume in lake or reservoir i (m^3); and $k_{m,i}$ is the (pseudo-) first order rate constant for loss process m in lake or reservoir i (s^{-1}).

Individual loss rate constants are extrapolated from test to field conditions by accounting for temperature differences, sorption to suspended solids and dissolved organic carbon,³² and

reduced light intensity.³³ Local sedimentation and volatilization rate constants are implemented via mass transport velocities between media.³⁴ Detailed information on the extrapolation to field conditions can be found in Supporting Information S3.

For characterization of annual mean flow, and highest and lowest monthly mean flow, the recent global FLO1K dataset was implemented in ePiE.²² FLO1K is based on an ensemble of artificial neural networks regressions, with upstream-catchment physiography (area, slope, elevation) and year-specific climatic variables (precipitation, temperature, potential evapotranspiration, aridity index and seasonality indices) as covariates. It provides estimations of flow at a spatial resolution of 30 arc seconds (~1 km) for the years 1960-2015, which are in good agreement with independent data (global R^2 of single-year metrics up to 0.91). An additional comparison with independent data obtained from 1,007 European monitoring stations for the period 2010-2015,³⁵ showed that year-specific annual mean flow, and highest and lowest mean monthly flow in European rivers are predicted well, with R^2 values of 0.97, 0.95 and 0.91, respectively (Figure 1).

Additional hydrological parameters flow velocity v_i (m/s) and river depth $h_{w,i}$ (m), were calculated via the Manning's equation for open channel flow, rewritten under the assumption of a wide rectangular river cross section as proposed by Pistocchi and Pennington.³⁶ In this approach, river width was related to river flow using their power law equation for European rivers (R^2 of 0.87).³⁶

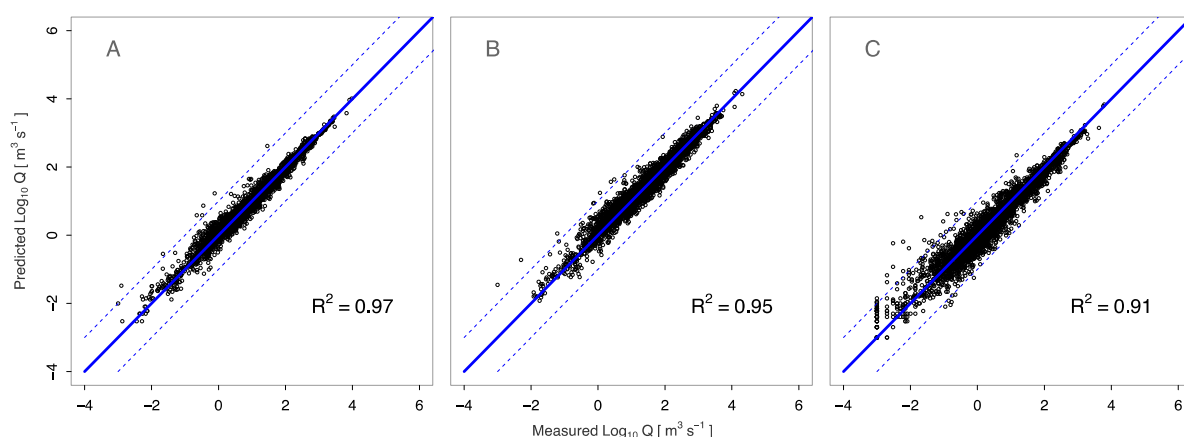


Figure 1. Validation results for year-specific annual mean flow (A), highest monthly mean flow (B) and lowest monthly mean flow (C). Independent validation dataset consisted of yearly measurements (2010-2015) from 1,007 GRDC European stations. The solid line represents perfect model fit (1:1 line) and the dashed lines represent a difference of one order of magnitude.

Model evaluation

We performed a model evaluation exercise with measured concentrations for 35 APIs consumed in Europe and covering a wide range of pharmaceutical classes. Excretion, sorption and degradation data were extracted from open literature by cross-referencing a set of reviews on human metabolism, sludge sorption, sediment sorption, biodegradation and photolysis. The data obtained were supplemented with additional API-specific searches. The resulting dataset was extensive, containing a total of 430 sorption coefficients and 342 degradation rate constants, but not homogeneously distributed over the 35 APIs. Complete experimental datasets were available for 13 APIs, while 12 were missing data on at least one sorption process and 11 on at least one degradation process. No experimental sorption or degradation data were found for sitagliptin and triamterene. Missing sorption coefficients were substituted by combining default mass fractions of organic carbon for sludge³⁰ or sediments³⁷ with QSAR predictions of organic carbon-water partition coefficients.^{38, 39} Moreover, if only ready biodegradability screening test data were available, APIs were assigned a biodegradation rate constant as proposed by Jager et al.⁴⁰ When experimental degradation rate constants were lacking altogether, no degradation was assumed. Table S4.1

and Table S4.2 show the physicochemical and environmental fate properties of the 35 APIs, respectively.

Predicted environmental concentrations were compared with measured concentrations extracted from a database compiled by the German national environmental protection agency,⁵ and a limited number of more recent literature studies. Individual studies were included in the model evaluation if 1) measurements were performed after 2010, 2) measurement locations were provided, 3) at least 10 of our APIs were measured above their limit of detection at least 10% of the time, and 4) multiple consecutive measurements were performed over time. These criteria resulted in the selection of three literature studies, being those by Burns et al.,⁴¹ who measured APIs in the river Ouse basin in the United Kingdom, and by Ruff et al.⁴² and Munz et al.,⁴³ who both measured APIs in the river Rhine basin in North-western Europe (Figure 2). Burns et al.⁴¹ included a total of 30 of our preselected APIs in a monthly grab-sampling campaign throughout 2016. They reported the coordinates of their 11 sampling locations, of which six were located along the river Ouse and five along its tributary, the river Foss, and we integrated these as such into ePiE. The yearly average of the Burns et al.⁴¹ dataset was compared to the PEC obtained under annual mean flow conditions for 2015. Ruff et al.⁴² measured a total of 23 of our preselected APIs in a weekly flow-proportional composite sampling campaign during “a remarkably dry period with constant low flow conditions” in the early spring of 2011. To reflect these low flow conditions, we used PECs derived under lowest monthly mean flow for 2011 in the quantitative evaluation of model performance. Out of their 16 sampling locations, ten were sampling stations along the river Rhine, but their coordinates were not reported. We georeferenced these sampling locations based on the proximity of the cities mentioned by the authors to sampling stations

in the GRDC Station Catalogue.³⁵ In addition, they sampled six tributaries of the river Rhine. We assumed these were sampled directly before their confluence with the main river. Finally, Munz et al.⁴³ included a total of 11 of our preselected APIs in two distinct grab-sampling campaigns in 2013 and 2014. Their 24 sampling locations were split evenly over these two campaigns and were all located directly downstream of WWTPs in Switzerland. Two sampling locations outside the river Rhine basin were excluded from our model evaluation. Similar to Ruff et al.⁴², Munz et al.⁴³ explicitly chose their sampling times to capture low flow conditions. Therefore, we used PECs derived under lowest monthly mean flow conditions for 2013 (site 1-12) and 2014 (site 13-24).

For estimations in the river Ouse basin, we used consumption data for 2016 from the Prescription Cost Analysis.⁴⁴ For the river Rhine basin, consumption data for the Netherlands were obtained from the Dutch National Health Care Institute.⁴⁵ German, French and Swiss consumptions during the years of interest were mostly extrapolated from per capita consumption in other years.⁴⁶ Consumption data were not available for 5 APIs in France, 1 API in Switzerland, and all APIs in Austria, Belgium and Luxembourg. In these cases, we averaged the per capita consumption from the basin's other countries. All consumption data are presented in Supporting Information S5.

To assess the predictive accuracy of ePiE, we computed the median symmetric accuracy ξ per study included in the evaluation exercise (Equation 5).⁴⁷ This metric reflects the typical percentage error of the predictions compared to the measurements. For example, a ξ of 100% indicates that predicted concentrations will typically be within a factor of 2 of the measurements. Contrary to metrics based on scale-dependent errors (e.g., root-mean-square error RMSE), ξ assigns equal importance to deviations of the same order rather than the same

magnitude. This is especially relevant for our data where concentrations ranged from low ng/L to µg/L levels. In other words, a situation where the PEC is 1 ng/L and the MEC is 10 ng/L (absolute error 9 ng/L) receives an equal penalty to that where the PEC is 100 ng/L and the MEC is 1 µg/L (absolute error 900 ng/L). Moreover, since ξ bases on the median of the accuracy ratios of individual pairs of predictions and measurements, it penalizes under- and overpredictions equally. This is an advantage over the often-applied mean absolute percentage error MAPE, which penalizes overpredictions more heavily.⁴⁷

$$\xi = 100 \cdot (e^{[M(|\ln(PEC_i/MEC_i)|)]} - 1) \quad \text{Equation 5}$$

Additionally, we assessed the prediction bias of ePiE by computing the symmetric signed percentage bias (SSPB) (Equation 6), which is closely related to the median symmetric accuracy ξ .⁴⁷ The SSPB can be interpreted similarly to a mean percentage error, but is not affected by the likely asymmetry in the distribution of percentage error.

$$SSPB = 100 \cdot \text{sgn}(M(\ln(PEC_i/MEC_i))) \cdot (e^{[M(|\ln(PEC_i/MEC_i)|)]} - 1) \quad \text{Equation 6}$$

Model application

To illustrate the utility of the model, we applied ePiE to prioritise APIs in the Ouse river basin, the basin with the best model performance and most APIs included. Additional nodes were integrated into the network at evenly spaced one-kilometre distances, enabling a basin-wide prioritisation using geographically homogeneous aggregate statistics. In addition to a ranking based on concentrations, we ranked the APIs based on their potential risks to fish. For this we followed a similar method as Burns et al.,⁴⁸ based on the fish plasma model approach.^{49, 50} We extrapolated concentrations in surface water to concentrations in fish plasma using bioconcentration factors computed according to Fitzsimmons et al.⁵¹ for neutral compounds,

274 and Fu et al.⁵² for ionizing compounds. The latter were derived assuming a surface water pH
275 of 7.4.⁵³ Risk quotients (RQ) for fish were then calculated as the ratio of concentrations in fish
276 plasma over therapeutic concentrations in human plasma, which we obtained from the
277 MaPPFAST database.⁵⁴ A risk quotient exceeding 1 thus indicates that the concentration of
278 an API in surface water is expected to cause a pharmacological effect in fish, assuming
279 equivalent pharmacological activity as in humans.⁵⁵ Finally, to enable exploration of local
280 concentration and risk patterns, model results were geographically visualized as interactive
281 html-maps, using the leaflet package “leafletR” in the R environment.⁵⁶

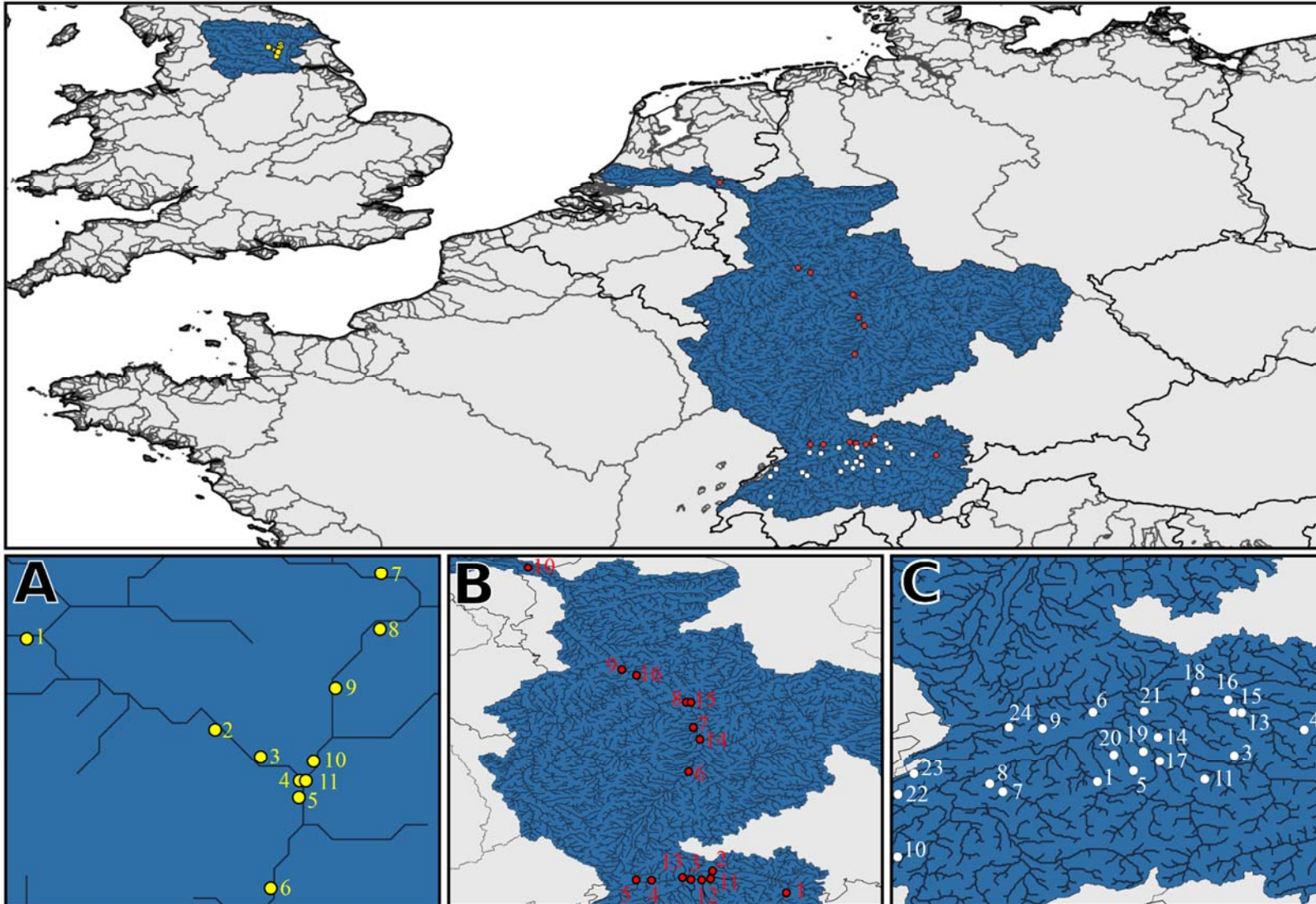


Figure 2. Overview of studies included in the model evaluation exercise, with numbered sampling locations from Burns et al.⁴¹ (A), Ruff et al.⁴² (B) and Munz et al.⁴³ (C).

Results and discussion

Out of the 940 predicted values used for model evaluation, 36% were qualified as non-detects in the measurement campaign. We qualified a substance as a non-detect in case it was below the limit of detection (LOD) in at least 40% of the samples taken at that location. Such non-detects are less suitable for a quantitative evaluation of model performance. We did, however, include them in a binary comparison between predicted min-max concentration ranges, resulting from the temporal variation in flow conditions, and measurements in relation to their LOD (Figure 3). Assigning comparisons to one of 4 bins (detected, predicted<LOD; not detected, predicted>LOD; detected, predicted>LOD; not detected, predicted<LOD), there was 94%, 88% and 90% coherence of predictions and measurements for the Burns et al.,⁴¹ Ruff et al.,⁴² and Munz et al.⁴³ studies, respectively (green bars in Figure 3).

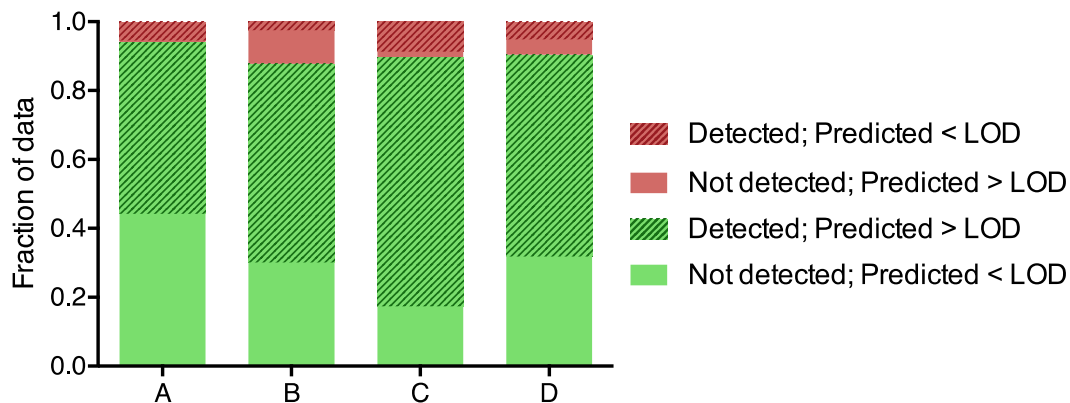


Figure 3. Binary comparison of measurements and min-max range of predictions, relative to their limit of detection (LOD). All combinations of location and API from Burns et al.⁴¹ (A), Ruff et al.⁴² (B), Munz et al.⁴³ (C), and all studies combined (D).

For a quantitative assessment of model performance, we included all detects at locations downstream of a WWTP, i.e., for which $PEC > 0$. In case measured values were below the LOD (i.e. always less than 40%), these measurements were replaced by $\frac{1}{2}\sqrt{2} \cdot LOD$.⁴⁸ The resulting comparison of predicted versus measured values (Figure 4) revealed a substantial variation

between the three studies. Model accuracy was best for predictions in the Ouse river basin, with a typical percentage error of 86% (Figure 4A; Burns et al.⁴¹). Predictions in the river Rhine basin had typical percentage errors of 143% (Figure 4B; Ruff et al.⁴²) and 158% (Figure 4C; Munz et al.⁴³). Model performance was similar if data points were included for which PEC>LOD and for which more than 40% of the measurements were below the LOD (Figure S6.1).

The worse performance of ePiE in the river Rhine basin might relate to the quality of the consumption data used in the calculations. Firstly, Swiss and German consumption data were often reported as “greater-than” values instead of exact amounts.⁴⁶ Secondly, we extrapolated the consumption in 2009 to that in the actual years of sampling (2011-2014), based on changing demographics and the assumption of a constant per capita consumption over the years (Table S5.1). However, actual per capita consumption has increased significantly for at least some pharmaceuticals, e.g., antidiabetics like sitagliptin⁵⁷ or antidepressants like venlafaxine.⁵⁸ These were therefore underestimated by ePiE due to the temporal extrapolation. In addition, errors might have been introduced when sampling sites from Ruff et al.⁴² were allocated to the river network, because limited geographical detail was available on their specific locations. Inaccuracies may also be due to the fact that HydroSHEDS does not provide the real geometry of a river network in a basin, but most likely flow paths between individual cells according to flow accumulation. Similarly, errors might have been introduced during the allocation to the river network of the WWTPs sampled by Munz et al.⁴³ These were all located at smaller streams in the upper Swiss catchment of the Rhine river basin, without other upstream emission sources. In such smaller upstream catchments, proximity-based allocation is more prone to errors because the main stream within the

floodplain is less easily identified. Nevertheless, the ξ values and the scatterplots in Figure 4 indicate that concentrations were typically predicted within a factor of 2-3, with approximately 95% of predictions within a factor of 10.

Concentrations measured by Burns et al.⁴¹ were typically underestimated by ePiE, with a symmetric signed percentage bias (SSPB) of -44% (Figure 4A). From the scatterplot in Figure 4A, underestimations seem to be more prominent at lower concentrations. This can at least partly be explained by the fact that measured concentrations have a lower bound in the form of their LOD, while model predictions do not. As a consequence, underestimations are more likely than overestimations in the vicinity of that LOD, since non-detects are excluded from the comparison. Indeed, model performance slightly improved if data points were included for which $PEC > LOD$, and which had more than 40% of the measurements below the LOD which were replaced by $\frac{1}{2}\sqrt{2} \cdot LOD$ (Figure S6.1). Additionally, the reliability of measured concentrations decreases closer to the LOD. This complicates the evaluation of model performance, because any difference between predicted and measured concentrations might then be attributed to errors in either of them. Finally, inputs from tourism, specific point sources (e.g., hospitals), operation of combined sewer overflows at selected times of the year and use of over the counter medicines may also explain the slight mismatch between measurements and predictions in the river Ouse basin.

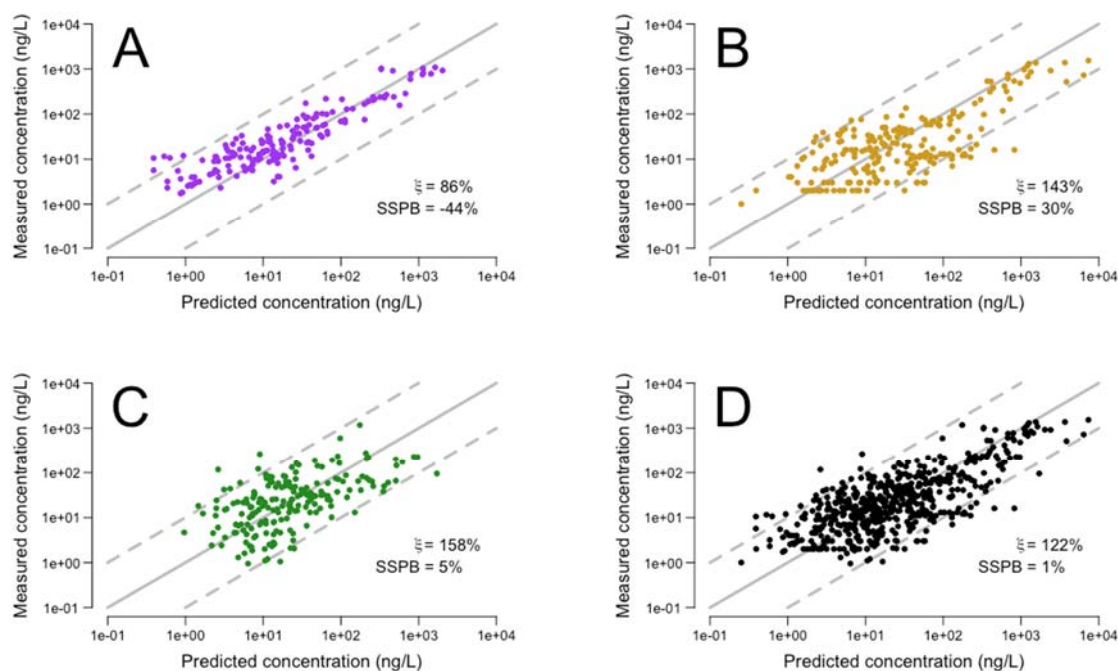


Figure 4. Predicted concentrations (i.e., >0) versus detects (i.e., <40% of the measurements below LOD), separately for data from Burns et al.⁴¹ (purple; A), Ruff et al.⁴² (golden; B), Munz et al.⁴³ (green; C), and for all studies combined (black; D). Concentrations predicted under annual mean flow conditions (A) or lowest monthly mean flow conditions (B and C). Solid line represents 1:1 relationship; dashed lines represent 1:10 and 10:1 relationships. ξ : median symmetric accuracy; SSPB: symmetric signed percentage bias.

In contrast to the river Ouse basin, concentrations measured in the river Rhine basin were typically slightly overestimated, with SSPB values of 30% and 5% (Figures 4B and 4C). When we ran ePiE under annual mean flow settings, these values dropped considerably to -70% and -313%, respectively. This indicates that actual streamflow during sampling was probably somewhere between lowest monthly mean flow and annual mean flow conditions.

Ratios of predicted over measured concentrations (PEC/MEC ratios) provide further insights into the performance of ePiE (Figure 5). PEC/MEC ratios are grouped according to study and sampling location, numbered as in Figure 2. Similar graphs grouped according to API are included in the Supporting Information (Figure S6.2). Figure 5A shows that the spread around predictions in the river Ouse (locations 1-6) is smaller than around those in its tributary river

380 Foss (locations 7-11). This indicates that ePiE predicts concentrations in larger rivers better
381 than in smaller ones. While concentrations in larger rivers reflect an accumulation of APIs
382 over a larger upstream catchment area, concentrations in smaller rivers and streams are more
383 directly influenced by specific local conditions, i.e. water extraction and retention or small
384 scale discharges. Indeed, comparison of predicted and measured mean annual flow at two
385 gauging stations, i.e. one in the river Ouse and one in the river Foss (Table S6.1), shows that
386 our flow prediction is less accurate for the smaller river Foss. The impact of local conditions
387 can furthermore be observed at the most upstream location on the river Foss (location 7),
388 where multiple APIs were detected but ePiE predicted zero concentrations for all of them.
389 This deviation was likely due to the presence of a small upstream WWTP not included in the
390 UWWTD-Waterbase because its size was below the reporting threshold of 2,000 p.e. National
391 consumption data and default WWTP characteristics might thus not always suffice to
392 estimate concentrations in locally influenced rivers. The same likely holds for the tributaries
393 of the river Rhine sampled by Ruff et al.⁴² (locations 11-16) and by Munz et al.⁴³ However, the
394 pattern is less obvious here, probably due to errors introduced by the aforementioned
395 incoherent flow conditions, consumption data, and geographical detail on sampling locations
396 and emission sources. One option to improve predictions in upstream tributaries is to extend
397 the UWWTD-Waterbase with WWTPs smaller than 2,000 p.e.

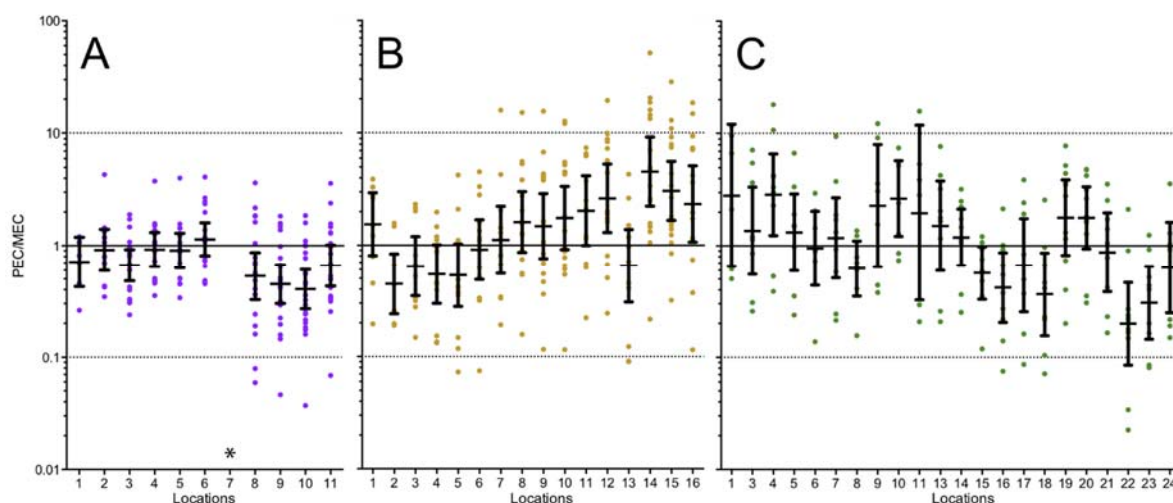


Figure 5. Ratios of predicted over measured concentrations (PEC/MEC), reported by Burns et al.,⁴¹ (A), Ruff et al.,⁴² (B) and Munz et al.⁴³ (C). Coloured dots are individual combinations of API and location, measured above the LOD; black bars represent 95th percentile and median over all measurements per location (numbered as in Figure 2). Concentrations predicted under annual mean flow conditions (A) or lowest monthly mean flow conditions (B and C). * = The PEC/MEC ratio of location 7 in panel A equals zero.

Figure 6A shows that predicted concentrations in the river Ouse basin were highest for metformin, gabapentin and acetaminophen, mainly resulting from their large consumption volumes, high excretion fractions and/or relatively poor degradation (Supporting Information S4.2 & S5). The prioritisation of APIs shifts when based on potential risks to fish instead of concentrations (Figure 6B). Metformin, gabapentin and acetaminophen drop down the list and are replaced by other more pharmacologically active APIs. Desvenlafaxine, loratadine and hydrocodone (highlighted in Figure 6A) then become APIs of particular interest. Their risk quotients for fish were larger than 0.1 in one or more locations in the river basin, with risk quotients for desvenlafaxine and loratadine even exceeding 1 in ~26% and ~10% of the river length, respectively. Interestingly, desvenlafaxine is formed as a metabolite of its prodrug venlafaxine but is not administered as a separate medication in the United Kingdom. This provides a strong argument for more focus on active metabolites in the environmental risk assessment of pharmaceuticals. Finally, Figure 7 shows that higher risks are mainly found in

417 more densely populated areas, e.g., around the city of Leeds. The geographical distribution
418 of surface water concentrations and risk quotients for all APIs is visualised in interactive html-
419 maps in Supporting Information S7.

420 Our model evaluation showed that ePiE generally predicts concentrations in surface waters
421 within one order of magnitude of measured concentrations for a wide range of
422 pharmaceutical classes. While other models have been shown to predict PECs of APIs to
423 within a factor 2-15 of measured concentrations,⁶⁰ none of these models have been evaluated
424 using such an extensive dataset on a diverse range of APIs. To further strengthen confidence
425 in the model, future model development and evaluation should extend towards additional,
426 more hydrologically and climatically diverse river basins. As part of the IMI funded project
427 iPiE, we are currently monitoring additional river basins in Denmark, Germany, Spain and the
428 UK to develop a broader dataset against which to evaluate the model. Because of its flexible
429 set-up and the use of global high-resolution gridded streamflow,²² ePiE can be extended to
430 new basins worldwide in a relatively straightforward way. Our model results also showed that
431 a proper assessment of model performance requires measured concentrations derived under
432 the same conditions as those modelled. This means that further model development should
433 ideally be supported by long-term annual sampling efforts. In addition, incorporation of local
434 consumption patterns, point sources (e.g., hospitals and pharmaceutical production plants),
435 WWTP characteristics, and environmental conditions, would be especially relevant for
436 adequate estimation of concentrations in smaller river stretches.

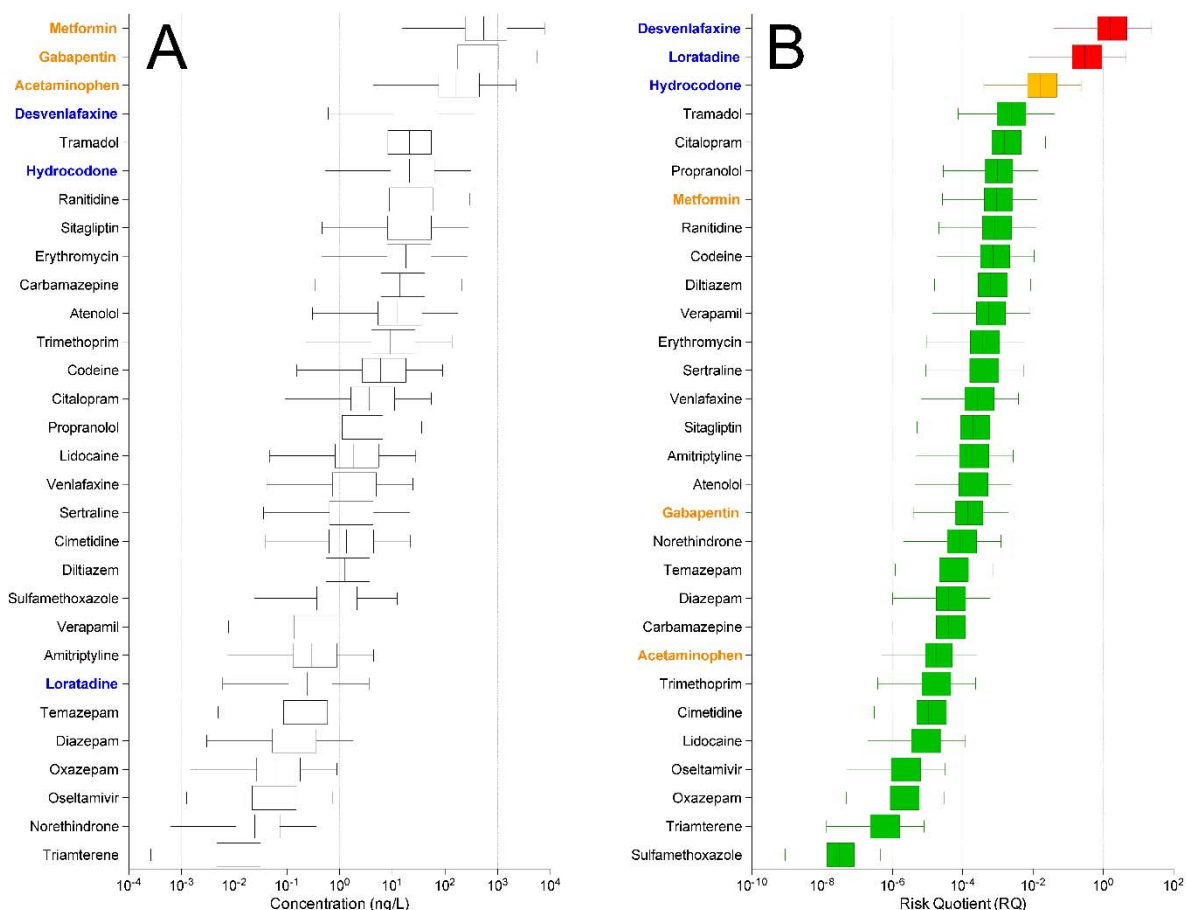


Figure 6. Ranking of all APIs modelled with ePiE in the Ouse river basin, based on concentrations (A) and risk quotients for fish (B) predicted throughout the river basin, excluding zero concentrations. Boxes indicate interquartile range including median; whiskers indicate 1st-99th percentile range for the total river length. Red boxes: RQ exceeds 1 at least somewhere in the river network; amber boxes: RQ exceeds 0.1 at least somewhere in the river network; green boxes: RQ below 0.1 throughout the river network.

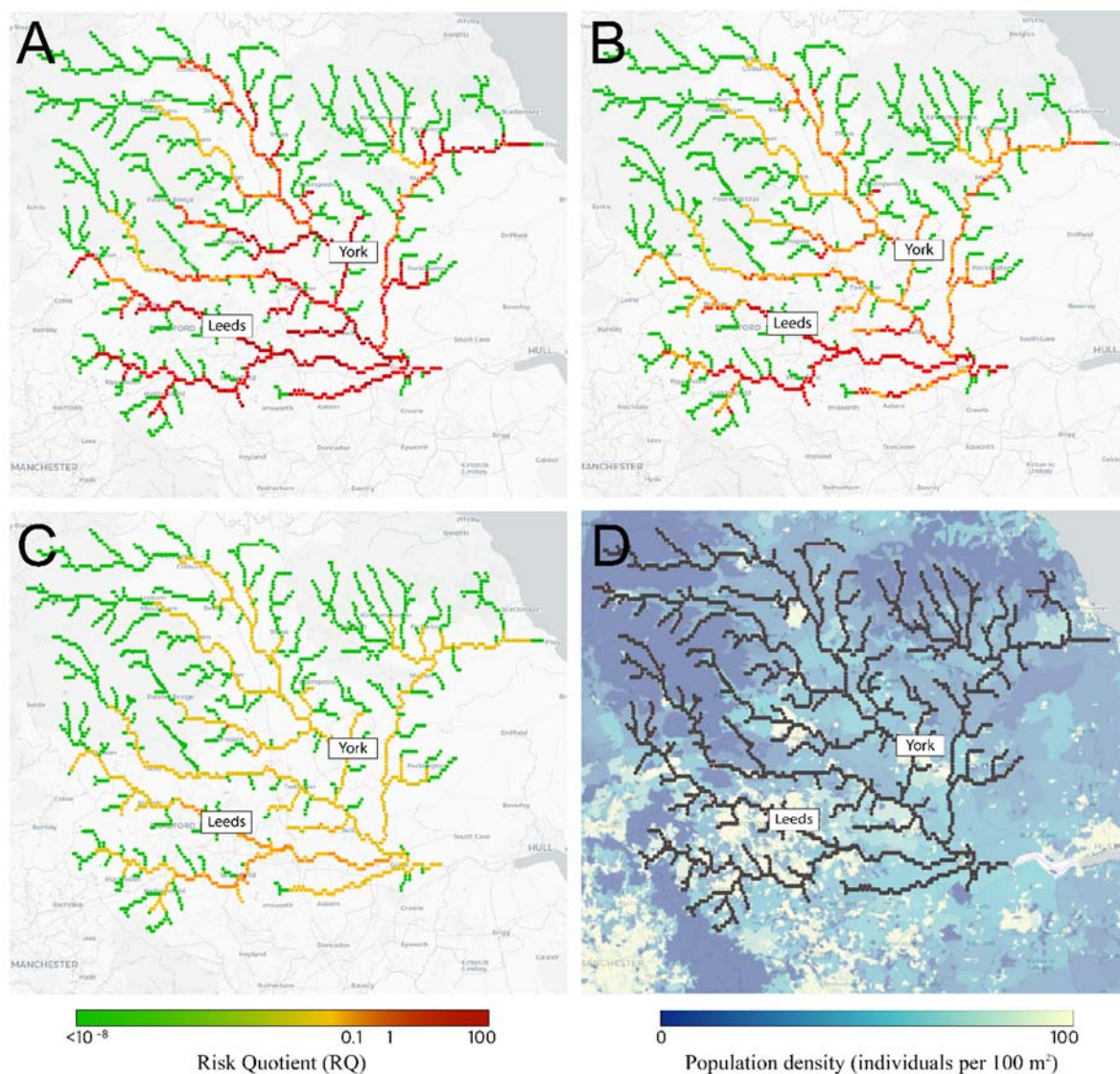


Figure 7. The spatial distribution of risk quotients for the three top ranked APIs in the river Ouse basin (UK): desvenlafaxine (A), loratadine (B), and hydrocodone(C). Panel D depicts the spatial variation in population density in the river Ouse basin (individuals/100 m²).

Supporting Information

S1. Curation of UWWTD-Waterbase

S2. Model construction

S3. Loss processes

S4. Chemical model parameterization

S5. Consumption data

S6. Additional results

S7. Interactive html-maps

Acknowledgments

The authors would like to thank John Wilkinson for his valuable contribution to the data collection and interpretation. This work was supported by the EU/EFPIA Innovative Medicines Initiative Joint Undertaking (iPiE Grant 115635).

References

1. Van Boeckel, T. P.; Gandra, S.; Ashok, A.; Caudron, Q.; Grenfell, B. T.; Levin, S. A.; Laxminarayan, R. Global antibiotic consumption 2000 to 2010: an analysis of national pharmaceutical sales data. *The Lancet Infectious Diseases* **2014**, *14* (8), 742-750.
2. Klein, E. Y.; Van Boeckel, T. P.; Martinez, E. M.; Pant, S.; Gandra, S.; Levin, S. A.; Goossens, H.; Laxminarayan, R. Global increase and geographic convergence in antibiotic consumption between 2000 and 2015. *Proceedings of the National Academy of Sciences* **2018**, *115* (15), E3463-E3470..
3. Jakimska, A.; Kot-Wasik, A.; Namieśnik, J. The Current State-of-the-Art in the Determination of Pharmaceutical Residues in Environmental Matrices Using Hyphenated Techniques. *Critical Reviews in Analytical Chemistry* **2014**, *44* (3), 277-298.

- 470 4. Noguera-Oviedo, K.; Aga, D. S. Lessons learned from more than two decades of
471 research on emerging contaminants in the environment. *Journal of Hazardous Materials*
472 **2016**, *316*, 242-251.
- 473 5. aus der Beek, T.; Weber, F.-A.; Bergmann, A.; Hickmann, S.; Ebert, I.; Hein, A.; Küster,
474 A. Pharmaceuticals in the environment—Global occurrences and perspectives. *Environmental*
475 *Toxicology and Chemistry* **2016**, *35* (4), 823-835.
- 476 6. Hughes, S. R.; Kay, P.; Brown, L. E. Global Synthesis and Critical Evaluation of
477 Pharmaceutical Data Sets Collected from River Systems. *Environmental Science & Technology*
478 **2013**, *47* (2), 661-677.
- 479 7. Daughton, C. G. The Matthew Effect and widely prescribed pharmaceuticals lacking
480 environmental monitoring: Case study of an exposure-assessment vulnerability. *Science of*
481 *The Total Environment* **2014**, *466*, 315-325.
- 482 8. Kinch, M. S.; Haynesworth, A.; Kinch, S. L.; Hoyer, D. An overview of FDA-approved
483 new molecular entities: 1827–2013. *Drug Discovery Today* **2014**, *19* (8), 1033-1039.
- 484 9. Overington, J. P.; Al-Lazikani, B.; Hopkins, A. L. How many drug targets are there?
485 *Nature Reviews Drug Discovery* **2006**, *5* (12), 993.
- 486 10. Boxall, A.; Rudd, M. A.; Brooks, B. W.; Caldwell, D. J.; Choi, K.; Hickmann, S.; Innes, E.;
487 Ostapyk, K.; Staveley, J. P.; Verslycke, T. Pharmaceuticals and personal care products in the
488 environment: what are the big questions? *Environmental health perspectives* **2012**, *120* (9),
489 1221-1229.
- 490 11. Oldenkamp, R.; Huijbregts, M. A. J.; Hollander, A.; Versporten, A.; Goossens, H.; Ragas,
491 A. M. J. Spatially explicit prioritization of human antibiotics and antineoplastics in Europe.
492 *Environment International* **2013**, *51* (0), 13-26.

- 493 12. Oldenkamp, R.; Huijbregts, M. A. J.; Ragas, A. M. J. The influence of uncertainty and
494 location-specific conditions on the environmental prioritisation of human pharmaceuticals in
495 Europe. *Environment International* **2016**, *91*, 301-311.
- 496 13. Vermeire, T.; Rikken, M.; Attias, L.; Boccardi, P.; Boeije, G.; Brooke, D.; de Bruijn, J.;
497 Comber, M.; Dolan, B.; Fischer, S.; Heinemeyer, G.; Koch, V.; Lijzen, J.; Müller, B.; Murray-
498 Smith, R.; Tadeo, J. European union system for the evaluation of substances: the second
499 version. *Chemosphere* **2005**, *59* (4), 473-485.
- 500 14. Pistocchi, A.; Sarigiannis, D. A.; Vizcaino, P. Spatially explicit multimedia fate models
501 for pollutants in Europe: State of the art and perspectives. *Science of The Total Environment*
502 **2010**, *408* (18), 3817-3830.
- 503 15. Grill, G.; Khan, U.; Lehner, B.; Nicell, J.; Ariwi, J. Risk assessment of down-the-drain
504 chemicals at large spatial scales: Model development and application to contaminants
505 originating from urban areas in the Saint Lawrence River Basin. *Science of The Total*
506 *Environment* **2016**, *541*, 825-838.
- 507 16. Żukowska, B.; Breivik, K.; Wania, F. Evaluating the environmental fate of
508 pharmaceuticals using a level III model based on poly-parameter linear free energy
509 relationships. *Science of The Total Environment* **2006**, *359* (1–3), 177-187.
- 510 17. Feijtel, T.; Boeije, G.; Matthies, M.; Young, A.; Morris, G.; Gandolfi, C.; Hansen, B.; Fox,
511 K.; Holt, M.; Koch, V.; Schroder, R.; Cassani, G.; Schowanek, D.; Rosenblom, J.; Niessen, H.
512 Development of a geography-referenced regional exposure assessment tool for European
513 rivers - great-er contribution to great-er #1. *Chemosphere* **1997**, *34* (11), 2351-2373.
- 514 18. Anderson, P. D.; D'Aco, V. J.; Shanahan, P.; Chapra, S. C.; Buzby, M. E.; Cunningham, V.
515 L.; DuPlessie, B. M.; Hayes, E. P.; Mastrocco, F. J.; Parke, N. J.; Rader, J. C.; Samuelian, J. H.;

516 Schwab, B. W. Screening Analysis of Human Pharmaceutical Compounds in U.S. Surface
 517 Waters. *Environmental Science & Technology* **2004**, 38 (3), 838-849.

518 19. Dumont, E.; Williams, R.; Keller, V.; Voß, A.; Tattari, S. Modelling indicators of water
 519 security, water pollution and aquatic biodiversity in Europe. *Hydrological Sciences Journal*
 520 **2012**, 57 (7), 1378-1403.

521 20. Williams, R. J.; Keller, V. D. J.; Johnson, A. C.; Young, A. R.; Holmes, M. G. R.; Wells, C.;
 522 Gross-Sorokin, M.; Benstead, R. A national risk assessment for intersex in fish arising from
 523 steroid estrogens. *Environmental Toxicology and Chemistry* **2009**, 28 (1), 220-230.

524 21. Kapo, K. E.; DeLeo, P. C.; Vamshi, R.; Holmes, C. M.; Ferrer, D.; Dyer, S. D.; Wang, X.;
 525 White-Hull, C. iSTREEM®: An approach for broad-scale in-stream exposure assessment of
 526 “down-the-drain” chemicals. *Integrated Environmental Assessment and Management* **2016**,
 527 12 (4), 782-792.

528 22. Barbarossa, V.; Huijbregts, M. A. J.; Beusen, A. H. W.; Beck, H. E.; King, H.; Schipper, A.
 529 M. FLO1K, global maps of mean, maximum and minimum annual streamflow at 1 km
 530 resolution from 1960 through 2015. *Scientific Data* **2018**, 5, 180052.

531 23. Bierkens, M. F. P. Global hydrology 2015: State, trends, and directions. *Water*
 532 *Resources Research* **2015**, 51 (7), 4923-4947.

533 24. Döll, P.; Douville, H.; Güntner, A.; Müller Schmied, H.; Wada, Y. Modelling Freshwater
 534 Resources at the Global Scale: Challenges and Prospects. *Surveys in Geophysics* **2016**, 37 (2),
 535 195-221.

536 25. Lehner, B.; Grill, G. Global river hydrography and network routing: baseline data and
 537 new approaches to study the world's large river systems. *Hydrological Processes* **2013**, 27
 538 (15), 2171-2186.

- 539 26. Lehner, B.; Verdin, K.; Jarvis, A. New global hydrography derived from spaceborne
540 elevation data. *Eos, Transactions American Geophysical Union* **2008**, 89 (10), 93-94.
- 541 27. Messenger, M. L.; Lehner, B.; Grill, G.; Nedeva, I.; Schmitt, O. Estimating the volume and
542 age of water stored in global lakes using a geo-statistical approach. **2016**, 7, 13603.
- 543 28. European Environmental Agency, UWWTD-WaterBase. Available from:
544 [http://www.eea.europa.eu/data-and-maps/data/waterbase-uwtd-urban-waste-water-](http://www.eea.europa.eu/data-and-maps/data/waterbase-uwtd-urban-waste-water-treatment-directive-4)
545 [treatment-directive-4](http://www.eea.europa.eu/data-and-maps/data/waterbase-uwtd-urban-waste-water-treatment-directive-4). Latest update at 19 February 2015.
- 546 29. Development Core Team. R: A Language and Environment for Statistical Computing. R
547 Foundation for Statistical Computing, Vienna, Austria.
- 548 30. Struijs, J. *SimpleTreat 4.0: a model to predict fate and emission of chemicals in*
549 *wastewater treatment plants*; National Institute for Public Health and the Environment:
550 Bilthoven, the Netherlands, 2014.
- 551 31. Lautz, L. S.; Struijs, J.; Nolte, T. M.; Breure, A. M.; van der Grinten, E.; van de Meent,
552 D.; van Zelm, R. Evaluation of SimpleTreat 4.0: Simulations of pharmaceutical removal in
553 wastewater treatment plant facilities. *Chemosphere* **2017**, 168, 870-876.
- 554 32. Honti, M.; Hahn, S.; Hennecke, D.; Junker, T.; Shrestha, P.; Fenner, K. Bridging across
555 OECD 308 and 309 Data in Search of a Robust Biotransformation Indicator. *Environmental*
556 *Science & Technology* **2016**, 50 (13), 6865-6872.
- 557 33. Schwarzenbach, R. P.; Gschwend, P. M.; Imboden, D. M. Photochemical
558 transformation reactions. In *Environmental organic chemistry*, Wiley-Interscience: New York,
559 New York, USA, 1993; pp 436-484.
- 560 34. Margni, M.; Pennington, D. W.; Bennett, D. H.; Jolliet, O. Cyclic Exchanges and Level of
561 Coupling between Environmental Media: Intermedia Feedback in Multimedia Fate Models.
562 *Environmental Science & Technology* **2004**, 38 (20), 5450-5457.

- 563 35. GRDC *Long-Term Mean Monthly Discharges and Annual Characteristics of GRDC*
564 *Stations / Global Runoff Data Centre.* ; Federal Institute of Hydrology (BfG). : Koblenz,
565 Germany, 2015.
- 566 36. Pistocchi, A.; Pennington, D. European hydraulic geometries for continental SCALE
567 environmental modelling. *Journal of Hydrology* **2006**, 329 (3–4), 553-567.
- 568 37. Fantke, P.; Bijster, M.; Guignard, C.; Hauschild, M.; Huijbregts, M.; Joliet, O.; Kounina,
569 A.; Magaud, V.; Margni, M.; McKone, T. E.; Posthuma, L.; Rosenbaum, R. K.; van de Meent, D.;
570 van Zelm, R. *USEtox (R) 2.0 Documentation (Version 1)*, <http://usetox.org>. *USEtox (R) is a*
571 *registered trademark of the USEtox (R) Team in the European Union and the United States. All*
572 *rights reserved. (C) USEtox (R) Team.* 2016.
- 573 38. Franco, A.; Trapp, S. Estimation of the soil–water partition coefficient normalized to
574 organic carbon for ionizable organic chemicals. *Environmental Toxicology and Chemistry*
575 **2008**, 27 (10), 1995-2004.
- 576 39. Sabljíć, A.; Güsten, H.; Verhaar, H.; Hermens, J. QSAR modelling of soil sorption.
577 Improvements and systematics of log KOC vs. log KOW correlations. *Chemosphere* **1995**, 31
578 (11), 4489-4514.
- 579 40. Jager, T.; Vermeire, T. G.; Rikken, M. G. J.; van der Poel, P. Opportunities for a
580 probabilistic risk assessment of chemicals in the European Union. *Chemosphere* **2001**, 43 (2),
581 257-264.
- 582 41. Burns, E. E.; Carter, L. J.; Kolpin, D. W.; Thomas-Oates, J.; Boxall, A. B. A. Temporal and
583 spatial variation in pharmaceutical concentrations in an urban river system. *Water Research*
584 **2018**, 137, 72-85.
- 585 42. Ruff, M.; Mueller, M. S.; Loos, M.; Singer, H. P. Quantitative target and systematic non-
586 target analysis of polar organic micro-pollutants along the river Rhine using high-resolution

587 mass-spectrometry – Identification of unknown sources and compounds. *Water Research*
588 **2015**, 87, 145-154.

589 43. Munz, N. A.; Burdon, F. J.; de Zwart, D.; Junghans, M.; Melo, L.; Reyes, M.;
590 Schönenberger, U.; Singer, H. P.; Spycher, B.; Hollender, J.; Stamm, C. Pesticides drive risk of
591 micropollutants in wastewater-impacted streams during low flow conditions. *Water Research*
592 **2017**, 110, 366-377.

593 44. National Health Service, Prescription Cost Analysis Data [online], available at: <
594 [https://www.nhsbsa.nhs.uk/prescription-data/dispensing-data/prescription-cost-analysis-](https://www.nhsbsa.nhs.uk/prescription-data/dispensing-data/prescription-cost-analysis-pca-data)
595 [pca-data](https://www.nhsbsa.nhs.uk/prescription-data/dispensing-data/prescription-cost-analysis-pca-data)>, last accessed: 11 Dec., 2017. In 2017.

596 45. Zorginstituut Nederland, GIPdatabank; available at: <https://www.gipdatabank.nl>. In
597 2015.

598 46. Singer, H. P.; Wössner, A. E.; McArde, C. S.; Fenner, K. Rapid Screening for Exposure
599 to “Non-Target” Pharmaceuticals from Wastewater Effluents by Combining HRMS-Based
600 Suspect Screening and Exposure Modeling. *Environmental Science & Technology* **2016**, 50
601 (13), 6698-6707.

602 47. Morley, S. K.; Brito, T. V.; Welling, D. T. Measures of Model Performance Based On the
603 Log Accuracy Ratio. *Space Weather* **2018**, 16 (1), 69-88.

604 48. Burns, E. E.; Thomas-Oates, J.; Kolpin, D. W.; Furlong, E. T.; Boxall, A. B. A. Are exposure
605 predictions, used for the prioritization of pharmaceuticals in the environment, fit for
606 purpose? *Environmental Toxicology and Chemistry* **2017**, 36 (10), 2823-2832.

607 49. Huggett, D. B.; Cook, J. C.; Ericson, J. F.; Williams, R. T. A Theoretical Model for Utilizing
608 Mammalian Pharmacology and Safety Data to Prioritize Potential Impacts of Human
609 Pharmaceuticals to Fish. *Human and Ecological Risk Assessment: An International Journal*
610 **2003**, 9 (7), 1789-1799.

- 611 50. Schreiber, R.; Gündel, U.; Franz, S.; Küster, A.; Rechenberg, B.; Altenburger, R. Using
612 the fish plasma model for comparative hazard identification for pharmaceuticals in the
613 environment by extrapolation from human therapeutic data. *Regulatory Toxicology and*
614 *Pharmacology* **2011**, *61* (3), 261-275.
- 615 51. Fitzsimmons, P. N.; Fernandez, J. D.; Hoffman, A. D.; Butterworth, B. C.; Nichols, J. W.
616 Branchial elimination of superhydrophobic organic compounds by rainbow trout
617 (*Oncorhynchus mykiss*). *Aquatic Toxicology* **2001**, *55* (1), 23-34.
- 618 52. Fu, W.; Franco, A.; Trapp, S. Methods for estimating the bioconcentration factor of
619 ionizable organic chemicals. *Environmental Toxicology and Chemistry* **2009**, *28* (7), 1372-
620 1379.
- 621 53. Meybeck, M.; Friedrich, G.; Thomas, R.; Chapman, D., Rivers. In *Water Quality*
622 *Assessments - A Guide to Use of Biota, Sediments and Water in Environmental Monitoring*, 2nd
623 ed.; Chapman, D., Ed. UNESCO/WHO/UNEP: 1996.
- 624 54. Berninger, J. P.; LaLone, C. A.; Villeneuve, D. L.; Ankley, G. T. Prioritization of
625 pharmaceuticals for potential environmental hazard through leveraging a large-scale
626 mammalian pharmacological dataset. *Environmental Toxicology and Chemistry* **2016**, *35* (4),
627 1007-1020.
- 628 55. Fick, J.; Lindberg, R. H.; Tysklind, M.; Larsson, D. G. J. Predicted critical environmental
629 concentrations for 500 pharmaceuticals. *Regulatory Toxicology and Pharmacology* **2010**, *58*
630 (3), 516-523.
- 631 56. Graul, C. leafletR: Interactive Web-Maps Based on the Leaflet JavaScript Library. R
632 package version 0.4-0, <http://cran.r-project.org/package=leafletR>. In 2016.

- 633 57. Guariguata, L.; Whiting, D. R.; Hambleton, I.; Beagley, J.; Linnenkamp, U.; Shaw, J. E.
634 Global estimates of diabetes prevalence for 2013 and projections for 2035. *Diabetes Research*
635 *and Clinical Practice* **2014**, *103* (2), 137-149.
- 636 58. Patten, S. B.; Williams, J. V. A.; Lavorato, D. H.; Bulloch, A. G. M.; Wiens, K.; Wang, J.
637 Why is major depression prevalence not changing? *Journal of Affective Disorders* **2016**, *190*,
638 93-97.
- 639 59. Neamțu, M.; Grandjean, D.; Sienkiewicz, A.; Le Faucheur, S.; Slaveykova, V.;
640 Colmenares, J. J. V.; Pulgarín, C.; de Alencastro, L. F. Degradation of eight relevant
641 micropollutants in different water matrices by neutral photo-Fenton process under UV254
642 and simulated solar light irradiation – A comparative study. *Applied Catalysis B:*
643 *Environmental* **2014**, *158–159*, 30-37.
- 644 60. Johnson, A. C.; Ternes, T.; Williams, R. J.; Sumpter, J. P. Assessing the Concentrations
645 of Polar Organic Microcontaminants from Point Sources in the Aquatic Environment: Measure
646 or Model? *Environmental Science & Technology* **2008**, *42* (15), 5390-5399.